

INCIDENCE RATE OF GRB-HOST-DLAS AT $Z = 1 - 10$ KENTARO NAGAMINE^{1,2}, BING ZHANG¹, LARS HERNQUIST³*Draft version October 12, 2021*

ABSTRACT

We study the incidence rate of damped Ly α systems associated with the host galaxies of gamma-ray bursts (GRB-HOST-DLAs) as functions of neutral hydrogen column density (N_{HI}) and projected star formation rate (SFR) using cosmological SPH simulations. Assuming that the occurrence of GRBs is correlated with the local SFR, we find that the median N_{HI} of GRB-HOST-DLAs progressively shifts to lower N_{HI} values with increasing redshift, and the incidence rate of GRB-HOST-DLAs with $\log N_{\text{HI}} > 21.0$ decreases rapidly at $z \geq 6$. Our results suggest that the likelihood of observing the signature of IGM attenuation in GRB afterglows increases towards higher redshift, because it will not be blocked by the red damping wing of DLAs in the GRB host galaxies. This enhances the prospects of using high-redshift GRBs to probe the reionization history of the Universe. The overall incidence rate of GRB-HOST-DLAs decreases monotonically with increasing redshift, whereas that of QSO-DLAs increases up to $z = 6$. A measurement of the difference between the two incidence rates would enable an estimation of the value of η_{GRB} , which is the mass fraction of stars that become GRBs for a given amount of star formation.

Subject headings: cosmology: theory — stars: formation — galaxies: evolution — galaxies: formation — methods: numerical

1. INTRODUCTION

A number of authors have proposed using GRBs to probe the history of cosmic star formation and the reionization of the Universe (e.g., Totani 1997; Miralda-Escude 1998; Lamb & Reichart 2000; Barkana & Loeb 2004), neither of which is well-understood (see, e.g., Holder et al. 2003; Nagamine et al. 2006). To date, observations of high-redshift (hereafter high- z) quasars and galaxies have been able to constrain reionization only up to $z \sim 7$ (Fan et al. 2006). However, if GRBs are associated with the deaths of massive stars (e.g., Woosley 1993; Paczynski 1998), then studies of early star formation (Schaefer et al. 2001; Abel et al. 2002; Bromm & Loeb 2006; Yoshida et al. 2006, 2007) imply that GRBs may be detectable out to $z \simeq 10 - 20$ through their prompt γ -ray emission and afterglows (Lamb & Reichart 2000; Ciardi & Loeb 2000; Gou et al. 2004; Inoue et al. 2007). This raises the possibility of using GRBs to investigate the reionization history of the Universe.

Observations with the Swift satellite have indeed led to the detection of high- z GRBs with bright afterglows (Cusumano et al. 2006). Analyses of the afterglow spectra, on the other hand, reveal the presence of damped Ly α systems in the red damping wing (Vreeswijk et al. 2004; Berger et al. 2006; Totani et al. 2006; Watson et al. 2006; Ruiz-Velasco et al. 2007). Compared with quasars, GRB lines-of-sight (LOSs) probe the central parts of galaxies (Prochaska et al. 2007) and are therefore often associated with neutral hydrogen (H I) absorption. This casts doubt on the use of

GRBs to constrain cosmic reionization (McQuinn et al. 2007). Thus, it is important to understand the redshift evolution of the incidence rate of GRB-HOST-DLAs at $z \geq 6$ as a function of N_{HI} .

In this *Letter*, we use cosmological SPH simulations based on the concordance Λ cold dark matter (CDM) model to study the N_{HI} distribution and the incidence rate of GRB-HOST-DLAs as a function of redshift between $z = 1 - 10$. The DLAs associated with quasar LOSs are often referred to as QSO-DLAs. Since quasars serve as randomly distributed background beacons in the Universe, QSO-DLAs can be more broadly interpreted as all the H I gas clouds that satisfy the DLA criterion ($N_{\text{HI}} > 2 \times 10^{20} \text{ cm}^{-2}$), regardless of whether or not they have been intersected by quasar LOSs. We adopt the latter broad interpretation of QSO-DLAs in this paper, and by this definition GRB-HOST-DLAs are a subset of QSO-DLAs.

2. SIMULATIONS

Our simulations were performed with the smoothed particle hydrodynamics (SPH) code GADGET-2 (Springel 2005), which includes radiative cooling by hydrogen and helium, heating by a uniform UV background (Katz et al. 1996; Davé et al. 1999), star formation and supernova feedback based on a sub-particle multiphase ISM model (Springel & Hernquist 2003a), and a phenomenological description of galactic winds (Springel & Hernquist 2003b).

Here, we use the Q5 & G5 runs from Springel & Hernquist (2003b), which have box sizes of 10 & 100 $h^{-1} \text{ Mpc}$, respectively. The total particle number is $N_p = 2 \times 324^3$ for gas and dark matter in each run. The initial gas particle mass is $m_{\text{gas}} = 3.3 \times 10^5 (3.3 \times 10^8) h^{-1} M_{\odot}$, the dark matter particle mass is $m_{\text{dm}} = 2.1 \times 10^6 (2.1 \times 10^9) h^{-1} M_{\odot}$, and the comoving gravitational softening length is 1.2 (8.0) $h^{-1} \text{ kpc}$ for

¹ University of Nevada Las Vegas, Department of Physics & Astronomy, 4505 Maryland Pkwy, Box 454002, Las Vegas, NV 89154-4002 U.S.A.; Email: kn@physics.unlv.edu

² Visitor, Institute for the Physics and Mathematics of the Universe, 5-1-5 Kashiwanoha Kashiwa-shi, Chiba 277-8582 Japan

³ Harvard University, 60 Garden Street, Cambridge, MA 02138, U.S.A.

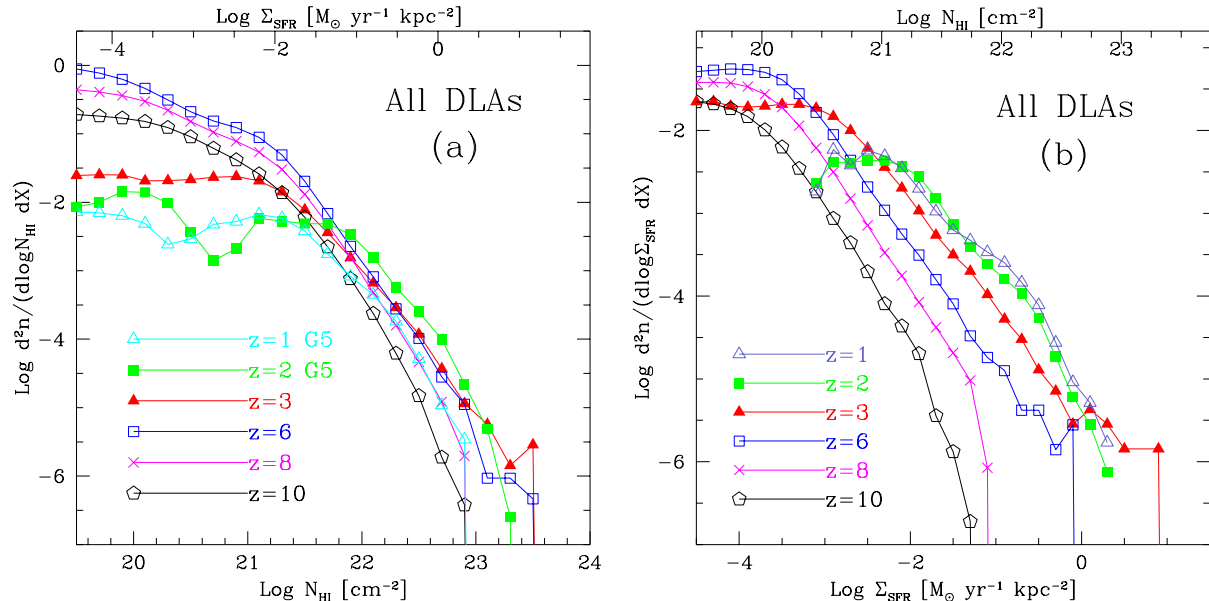


FIG. 1.— Distribution of all DLAs as a function of N_{HI} (panel [a]) and Σ_{SFR} (panel [b]) at $z = 1 - 10$. The Q5 run was used for $z > 3$, and the G5 run for $z < 3$. The top axis in each panel indicates corresponding values of N_{HI} and Σ_{SFR} based on the empirical Kennicutt (1998) law. Nagamine et al. (2004b) have shown that the simulated galaxies follow the Kennicutt law well.

the Q5 (G5) run. We use the Q5 run for $z > 3$ (for higher resolution), and the G5 run for $z < 3$ (for better sampling of more massive halos and longer wavelength perturbations).

Previously, we have used these simulations to study the properties of DLAs (Nagamine et al. 2004a,b, 2007), Ly-break galaxies at $z = 3 - 6$ (Nagamine et al. 2004c; Night et al. 2006), and Ly α emitters (Nagamine et al. 2008). In general, the simulations show good agreement with available galaxy observations, giving some confidence that we are capturing the basic aspects of hierarchical galaxy evolution in the context of the Λ CDM model. Moreover, the cosmic star formation history implied by the simulations (Hernquist & Springel 2003) agrees with observational estimates (Faucher-Giguere et al. 2008a) and supports the association of GRBs with massive star formation (Faucher-Giguere et al. 2008b). The adopted cosmological parameters of all simulations considered here are $(\Omega_m, \Omega_\Lambda, \Omega_b, \sigma_8, h) = (0.3, 0.7, 0.04, 0.9, 0.7)$, where $h = H_0/(100 \text{ km s}^{-1} \text{ Mpc}^{-1})$.

3. RESULTS

First, we present the distribution of all DLAs in the simulation as a function of N_{HI} in Figure 1a. The method of calculating N_{HI} in the simulations is described fully in Nagamine et al. (2004a). Briefly, we set up a cubic grid that covers each dark matter halo, and calculate N_{HI} by projecting the HI mass distribution onto one of the planes. The quantity “ dn ” is the area covering fraction on the sky along the line element cdt (see Eqns. 5–7 of Nagamine et al. 2007), and the function $d^2n/(d \log N_{\text{HI}} dX) = f(N_{\text{HI}}, X) N_{\text{HI}} \ln(10)$ is the ‘incidence rate’ per unit $\log N_{\text{HI}}$ and per unit absorption distance $X(z)$, where $dX = \frac{H_0}{H(z)}(1+z)^2 dz$. The function $f(N_{\text{HI}}, X)$ is usually referred to as the column density distribution function.

Figure 1a shows that, from $z = 10$ to $z = 6$, the incidence rate increases monotonically with decreasing redshift at all N_{HI} , reflecting the rapidly growing number of dark matter halos. From $z = 6$ to $z = 3$, there is not much change at $\log N_{\text{HI}} > 22$, but the number of columns at $\log N_{\text{HI}} < 21$ has decreased significantly, which could owe to the UV background radiation field imposed at $z = 6$ in the simulation to model reionization. From $z = 3$ to $z = 2$, the number of columns at $\log N_{\text{HI}} > 22$ increases, but it decreases from $z = 2$ to $z = 1$, owing to the conversion of high-density gas into stars.

If long GRBs are associated with the collapse of massive stars, then their occurrence should be correlated with the local SFR. Therefore we define the following to quantify the distribution of GRB-HOST-DLAs:

$$\zeta_{\text{GRB-HOST-DLA}} \equiv \frac{d^2n}{dX d \log \Sigma_{\text{SFR}}} \frac{\Sigma_{\text{SFR}}}{\langle \Sigma_{\text{SFR}} \rangle} \eta_{\text{GRB}}, \quad (1)$$

where Σ_{SFR} is the projected SFR in units of $[M_\odot \text{ yr}^{-1} \text{ kpc}^{-2}]$, and $\langle \Sigma_{\text{SFR}} \rangle$ is a normalization parameter. Although it is somewhat arbitrary, we take $\langle \Sigma_{\text{SFR}} \rangle = 10^{-4}$, because it roughly corresponds to $\log N_{\text{HI}} \approx 20$ based on the Kennicutt (1998) law. The parameter η_{GRB} denotes the mass fraction of stars that become GRBs and have associated afterglows for a given amount of star formation with a certain stellar initial mass function (IMF). The exact value of η_{GRB} depends on the IMF and other GRB physics. Here, we take $\eta_{\text{GRB}} = 10^{-3}$, because the mass fraction of stars with $M > 8 M_\odot$ is 23% of the total for a Chabrier (2003) IMF with a mass range $[0.1, 100] M_\odot$, and the global average of the GRB/SN ratio is $\sim 0.5\%$ (Yoon et al. 2006; Soderberg 2007; Campana et al. 2008). If one takes the number fraction ($\sim 6\%$ for $M > 8 M_\odot$ stars) instead of the mass fraction in the above calculation, then $\eta_{\text{GRB}} = 3 \times 10^{-4}$. Here we use the mass fraction, because weighting by $\Sigma_{\text{SFR}}/\langle \Sigma_{\text{SFR}} \rangle$ is done on the basis of stellar mass.

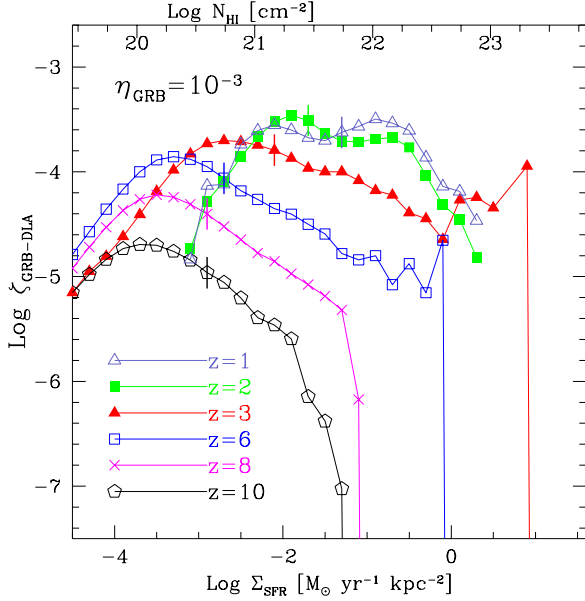


FIG. 2.— Distribution of GRB-HOST-DLAs as a function of N_{HI} at $z = 1 - 10$. The top axis shows the corresponding values of N_{HI} based on the empirical Kennicutt (1998) law, and the tick-marks indicate the median of the distribution for columns with $\log \Sigma_{\text{SFR}} > -3.3$ or $\approx \log N_{\text{HI}} > 20.3$.

In principle, one could absorb the factor $\langle \Sigma_{\text{SFR}} \rangle$ into η_{GRB} and treat them as one parameter: $\eta'_{\text{GRB}} \equiv \eta_{\text{GRB}} / \langle \Sigma_{\text{SFR}} \rangle$, which would be the GRB rate per projected SFR. However, here we choose to treat them separately to keep the physical meaning of η_{GRB} clear. In the future, GRB theory may be able to estimate the value of η_{GRB} , and observations of GRB-HOST-DLAs will constrain the ratio of $\eta_{\text{GRB}} / \langle \Sigma_{\text{SFR}} \rangle$ (see § 4 and 5).

It is worthwhile to look at the distribution $d^2n / (dX d \log \Sigma_{\text{SFR}})$, before weighting it by Σ_{SFR} . Figure 1b shows that the redshift evolution of this distribution is stronger than in Fig. 1a. The number of columns with $\log \Sigma_{\text{SFR}} \gtrsim -2.5$ ($\approx \log N_{\text{HI}} \gtrsim 21.0$ for the Kennicutt law) decreases systematically from $z = 1$ to $z = 10$.

Figure 2 shows $\zeta_{\text{GRB-HOST-DLA}}$ as a function of $\log \Sigma_{\text{SFR}}$. Because of the weighting by $\Sigma_{\text{SFR}} / \langle \Sigma_{\text{SFR}} \rangle$, the distribution now exhibits a peak with a broad tail at high Σ_{SFR} . The number of columns with $\log N_{\text{HI}} > 21$ decreases progressively from $z = 1$ to $z = 10$, owing to the decreasing number of massive dark matter halos with deep potential wells towards higher redshifts. This is encouraging for the use of GRB afterglows to probe reionization, because the IGM attenuation signature is less likely to be blocked by the red damping wing of GRB-HOST-DLAs. The median value of the distribution at $\log \Sigma_{\text{SFR}} > -3.3$ ($\approx \log N_{\text{HI}} > 20.3$ for the Kennicutt law) is $\log N_{\text{HI}} = -1.3, -1.7, -2.1, -2.7, -2.9$ & -2.9 for $z = 1, 2, 3, 6, 8$ & 10 , respectively. The distributions at $z = 1$ & 2 have broad peaks at $\log N_{\text{HI}} = 21.0 - 22.3$, which is consistent with observations (e.g., Jakobsson et al. 2006; Savaglio 2006; Prochaska et al. 2007). However, we note that the decline of the distribution at $\log \Sigma_{\text{SFR}} < -2.5$ for $z = 1$ & 2 may owe to the limited resolution of the G5 run compared to the Q5 run.

By integrating $\zeta_{\text{GRB-HOST-DLA}}$ over $\log \Sigma_{\text{SFR}}$,

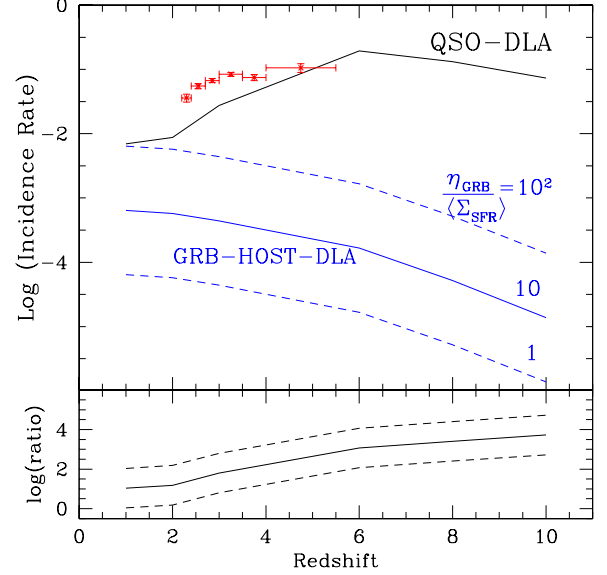


FIG. 3.— *Top panel:* Incidence rates of GRB-HOST-DLAs and QSO-DLAs as a function of redshift. (See text for the sources of the data points.) For GRB-HOST-DLAs, the three blue curves correspond to $\eta_{\text{GRB}} / \langle \Sigma_{\text{SFR}} \rangle = 10^2, 10$, & 1 from top to bottom. *Bottom panel:* Ratio of the two incidence rates.

we obtain the ‘incidence rate’ of GRB-HOST-DLAs. The integral at $\log \Sigma_{\text{SFR}} > -3.3$ yields rates of $(6.4, 5.7, 4.4, 1.7, 0.52, 0.14) \times 10^{-4}$ for $z = 1, 2, 3, 6, 8$ & 10 , respectively, for the assumed value of $\eta_{\text{GRB}} / \langle \Sigma_{\text{SFR}} \rangle = 10$. Figure 3 compares the derived incidence rate of GRB-HOST-DLAs to that of QSO-DLAs. The red data points are the updated version⁴ of Prochaska et al. (2005) using SDSS DR5. Our simulations somewhat underpredict the QSO-DLA incidence rate owing to the underestimate of $f(N_{\text{HI}})$ at $\log N_{\text{HI}} < 21$ (Nagamine et al. 2004a). There is a stark difference between the evolution of the two rates: the incidence rate of GRB-HOST-DLAs decreases monotonically towards high- z , whereas the QSO-DLA rate increases from $z = 1$ to $z = 6$. This is because we assumed that GRBs are correlated with star formation and their distribution is not random, unlike the background quasars. The offset between the QSO-DLA and GRB-HOST-DLA incidence rates tells us about the difference between the total HI cross section of galaxies and the area covering fraction of star-forming regions. The QSO-DLA sight-lines can also probe the outskirts of galaxies where star formation is nonexistent, therefore their incidence rate is much higher than that of GRB-HOST-DLAs.

4. PROBABILITY FOR A GIVEN GRB

Of immediate interest to GRB observers is the chance probability of finding a GRB-HOST-DLA for a given GRB event. For individual GRBs, the probability of having a GRB-HOST-DLA should depend on the geometry of the HI gas distribution around the GRB along the LOS. While our simulations do not have the resolution to follow the gas dynamics within molecular clouds, the Q5 run has a physical gravitational softening length of

⁴ <http://www.ucolick.org/~xavier/SDSSDLA/>

0.31 (0.18) h^{-1} kpc at $z = 3$ (6), and the gas distribution above these scales is followed reasonably well. The O and B stars would have ionized all the gas within ~ 100 pc of the GRB creating an HII region, thus we expect the DLA gas to be located at > 0.1 kpc from the GRB (Prochaska et al. 2007). Then, our simulations can follow the qualitative trend in the redshift evolution of the incidence rate of GRB-HOST-DLAs.

Since our simulations roughly match the Kennicutt law (Nagamine et al. 2004b), it is guaranteed that columns with $\log N_{\text{HI}} > 20.3$ will have star formation along the LOS. Therefore if long GRBs are associated with star formation as we have assumed, essentially all GRB events will have GRB-HOST-DLAs along their LOS. A more detailed analysis would be required to fully confirm this, by generating the absorption line profiles for each GRB LOS, and we plan to examine this in due course using higher resolution simulations.

Nevertheless, Figure 2 shows that the number of high- N_{HI} systems decreases with increasing redshift, and so we expect that the chance probability of having a high- N_{HI} DLA for a given GRB event will also decline towards high- z with a similar qualitative trend as shown in Figure 3. But we stress that the incidence rate shown in Figure 3 is *not* the probability of detecting a DLA for a given GRB.

5. CONCLUSIONS & DISCUSSIONS

Using cosmological SPH simulations, we have examined the redshift evolution of distribution functions and incidence rates of GRB-HOST-DLAs, assuming that long GRBs are correlated with the local SFR. The distribution of GRB-HOST-DLAs is intrinsically different from that of QSO-DLAs and we find that the incidence rate of GRB-HOST-DLAs decreases monotonically towards high- z , whereas the incidence rate of QSO-DLAs increases from $z = 1$ to $z = 6$. Quasars are assumed to be randomly distributed background sources in the sky which illuminate the DLA gas in foreground galaxies along the quasar LOS. GRBs can also serve as randomly distributed beacons with respect to the DLA gas in foreground galaxies, but for GRB-HOST-DLAs, GRBs are not random background sources because they are in the same host galaxy.

We find that the incidence rate of GRB-HOST-DLAs with $\log N_{\text{HI}} > 21.0$ decreases rapidly at $z \geq 6$, suggesting that the likelihood of observing the IGM attenuation signature in GRB afterglows increases toward higher redshifts, without being blocked by the red damping of DLAs in the GRB host galaxies. This enhances the prospects for using high- z GRBs to probe the reionization history of the Universe. Our predictions can

be tested by upcoming high- z GRB missions, including *JANUS* (*Joint Astrophysics Nascent Universe Scout*) and *SVOM* (*Space multi-band Variable Object Monitor*).

It might be hoped that it would be possible to estimate the incidence rate of GRB-HOST-DLAs by accumulating a large GRB sample. However, because GRBs are not random background sources for GRB-HOST-DLAs, this would require a prohibitively large sample of GRBs to estimate the area covering fraction of GRB-HOST-DLAs from GRB observations alone. If long GRBs do indeed trace star-forming regions as we have assumed, and if all the LOSs to star-forming regions are coincident with DLAs, then one could estimate the total GRB-HOST-DLA incidence rate simply by measuring the area covering fraction of star-forming regions from deep imaging surveys of galaxies. When the number of GRBs becomes comparable to that of QSOs, one should expect non-negligible new intervening DLAs in GRB LOSs that are not associated with GRB hosts, since GRB afterglows now act as random beacons.

An alternative possibility would be to search for quasars in the proximity of GRBs, or vice versa. Such a search of QSO-GRB pair-LOSs would yield a coincidence probability between QSO-DLAs and GRB-HOST-DLAs, which roughly corresponds to the ratio of the two incidence rates. So far, no such cases have been identified, but a combination of all-sky GRB surveys (e.g., BATSE, Swift, GLAST) and optical-IR imaging surveys of galaxies (e.g., SDSS, Pan-STARRS, LSST) may prove successful in the future. A constraint on the ratio of the two incidence rates would make it possible to estimate the ratio $\eta_{\text{GRB}}/\Sigma_{\text{SFR}}$. In addition, deep observations of GRB host galaxies could constrain Σ_{SFR} independently. Then combining the above two constraints would allow us to estimate the value of η_{GRB} .

ACKNOWLEDGMENTS

This work is supported in part by the National Aeronautics and Space Administration under Grant/Cooperative Agreement No. NNX08AE57A issued by the Nevada NASA EPSCoR program. BZ acknowledges the support from the NASA grant NNG06GH62G. We acknowledge the significant contribution of Volker Springel for the simulations used in this work. KN is grateful for the hospitality of Institute for the Physics and Mathematics of the Universe (IPMU), where a part of this work was performed. The simulations were performed at the Institute of Theory and Computation at Harvard-Smithsonian Center for Astrophysics, and the analyses were performed at the UNLV Cosmology Computing Cluster.

REFERENCES

- Abel, T., Bryan, G. L., & Norman, M. L. 2002, *Science*, 295, 93
- Barkana, R. & Loeb, A. 2004, *ApJ*, 601, 64
- Berger, E., et al. 2006, *ApJ*, 642, 979
- Bromm, V. & Loeb, A. 2006, *ApJ*, 642, 382
- Campana, S., et al. 2008, arXiv:0805.4698
- Chabrier, G. 2003, *PASP*, 115, 763
- Ciardi, B. & Loeb, A. 2000, *ApJ*, 540, 687
- Cusumano, G., et al. 2006, *Nature*, 440, 164
- Davé, R., et al. 1999, *ApJ*, 511, 521
- Fan, X., Carilli, C. L., & Keating, B. 2006, *ARA&A*, 44, 415
- Faucher-Giguere, C., et al. 2008a, *ApJ*, in press, arXiv:0806.0372
- Faucher-Giguere, C., et al. 2008b, *ApJ*, submitted
- Gou, L. J., et al. 2004, *ApJ*, 604, 508
- Hernquist, L. & Springel, V. 2003, *MNRAS*, 341, 1253
- Holder, G. P., et al. 2003, *ApJ*, 595, 13
- Inoue, S., Omukai, K., & Ciardi, B. 2007, *MNRAS*, 380, 1715
- Jakobsson, P., et al. 2006, *A&A*, 460, L13
- Katz, N., Weinberg, D. H., & Hernquist, L. 1996, *ApJS*, 105, 19
- Kennicutt, R. C. J. 1998, *ApJ*, 498, 541
- Lamb, D. Q. & Reichart, D. E. 2000, *ApJ*, 536, 1
- McQuinn, M., et al. 2008, *MNRAS*, in press, arXiv:0710.1018
- Miralda-Escude, J. 1998, *ApJ*, 501, 15
- Nagamine, K., et al. 2006, *ApJ*, 653, 881
- Nagamine, K., et al. 2008, arXiv:0802.0228

- Nagamine, K., Springel, V., & Hernquist, L. 2004a, MNRAS, 348, 421
—. 2004b, MNRAS, 348, 435
Nagamine, K., et al. 2004c, MNRAS, 350, 385
Nagamine, K., et al. 2007, ApJ, 660, 945
Night, C., et al. 2006, MNRAS, 366, 705
Paczynski, B. 1998, ApJ, 494, L45
Prochaska, J. X., et al. 2007, ApJ, 666, 267
Prochaska, J. X., Herbert-Fort, S., & Wolfe, A. M. 2005, ApJ, 635, 123
Ruiz-Velasco, A. E., et al. 2007, ApJ, 669, 1
Savaglio, S. 2006, New Journal of Physics, 8, 195
Schaefer, B. E., Deng, M., & Band, D. L. 2001, ApJ, 563, L123
Soderberg, A. M. 2007, in American Institute of Physics Conference Series, Vol. 937, Supernova 1987A: 20 Years After: Supernovae and Gamma-Ray Bursters, ed. S. Immler & R. McCray, 492–499
Springel, V. 2005, MNRAS, 364, 1105
Springel, V. & Hernquist, L. 2003a, MNRAS, 339, 289
—. 2003b, MNRAS, 339, 312
Totani, T. 1997, ApJ, 486, L71
Totani, T., et al. 2006, PASJ, 58, 485
Vreeswijk, P. M., et al. 2004, A&A, 419, 927
Watson, D., et al. 2006, ApJ, 652, 1011
Woosley, S. E. 1993, ApJ, 405, 273
Yoon, S.-C., Langer, N., & Norman, C. 2006, A&A, 460, 199
Yoshida, N., et al. 2006, ApJ, 613, 406
Yoshida, N., Omukai, K., & Hernquist, L. 2007, ApJ, 667, 117